THESIS FOR DEGREE OF LICENTIATE OF ENGINEERING

Evolution of Powder Surface Chemistry and Powder Properties during Powder-based Metal Additive Manufacturing

SOFIA KAZI

Department of Industrial and Materials Science
CHALMERS UNIVERSITY OF
TECHNOLOGY Gothenburg, Sweden, 2025

EVOLUTION OF POWDER SURFACE CHEMISTRY AND POWDER PROPERTIES DURING POWDER-BASED METAL ADDITIVE MANUFACTURING

Sofia Kazi

Technical report No. IMS-2025-6

Department of Industrial and Materials Science Chalmers
University of Technology
SE-412-96 Gothenburg
Sweden
Tel: + 46 (0)31-772 1000
Email: sofiakaz@chalmers.se

Printed by Chalmers Reproservice
Gothenburg, Sweden, 202

Evolution of Powder Surface Chemistry and Powder Properties during Powder-based Metal Additive Manufacturing

Sofia Kazi
Department of Industrial and Materials Science
Chalmers University of Technology

Abstract

Powder-based additive manufacturing (AM) is a transformative technology enabling the fabrication of parts to near-net-shape through layer-by-layer deposition and selective consolidation of thin powder layers according to a digital 3D model. Due to their high surface area to volume ratio, powders are susceptible to surface reactions, particularly oxidation upon exposure to atmospheric oxygen and moisture. Complexity of these AM processes, such as printing atmosphere, interactions of the energy source with the powder particles, leading to "spatter" generation, as well as necessary post-printing steps can induce surface oxidation and alter the powder's physical properties. Even brief exposure during handling, storage, or within the build chamber can lead to the growth of oxide layer thickness on the powder particle surfaces. Different types of degradation phenomena in the powder feedstock can lead to defects in the final components, compromising their properties as well as the process repeatability. Therefore, this thesis aims to study the impact of powder reuse in AM on powder surface chemistry and powder properties.

When it comes to powder degradation in PBF-LB, reuse and recycling of 316L stainless steel powder were studied. The thickness of the oxide layer on the powder surface almost doubled after 140 hours of total in process exposure. Further on, recycling of the powder through atomization of 316L reused powder and AM scrap was successfully performed and allowed to achieve powder with chemistry and properties comparable to virgin 316L powder used in the study. In the second part, copper powder of high purity was employed for printing components for electromagnetic applications using PBF-EB. The powder proved to undergo varying surface chemistry changes depending on the process parameters used, with a transformation of the dominant CuO oxide on the surface of the virgin particles to Cu_2O after PBF-EB processing. Further on, changes in stainless steel 17-4 PH powder properties during reuse in BJT were studied. Conditioning of the powder was applied before the first print, which aided the particles' spreadability during the printing process. Post-printing steps to ensure the densification of the components, such as curing, led to a rise in oxide layer thickness of the powder, promoting instability of the printing process after 20 prints and multiple curing cycles.

Keywords: Additive Manufacturing; Powder Bed Fusion-Laser Beam; Powder Bed Fusion-Electron Beam; Binder Jetting; Surface Oxidation; 17-4 PH; Copper; 316L; Rheological Properties.

Preface

The presented work in the licentiate thesis was conducted at the Division of Material and Manufacture at the Department of Industrial Materials and Science, Chalmers University of Technology. The research was carried out in the frame of the Center for Additive Manufacturing – Metal (CAM^2), under the direct supervision of Prof. Eduard Hryha, with Prof. Lars Nyborg as the examiner.

List of appended papers

I. **Changes in Powder Surface Chemistry During Reuse of 316L in Powder Bed Fusion - Laser Beam**

__Sofia Kazi__, Lindsay Leach, Eduard Hryha

Proceedings of EuroPM2024 Conference, 2024, https://doi.org/10.59499/EP246282011

II. **Recycling of 316L Powder and Scrap from Additive Manufacturing Processing**

Liviu Brabie, __Sofia Kazi__, Annika Strondl, Pelle Mellin, Tatiana Fedina, Lindsay Leach, Eduard Hryha

Proceedings of EuroPM2024 Conference, 2024, https://doi.org/10.59499/EP246277177

III. **Changes in Powder Surface Chemistry During Reuse of Pure Copper in Powder Bed Fusion - Electron Beam**

__Sofia Kazi__, Phillip Mahoney, Eduard Hryha

Journal of the Japan Society of Powder and Powder Metallurgy, 2025, Vol. 72 (Supplement), pp. S593-597, https://doi.org/10.2497/jjspm.15C-T1-28

IV. **Exploring the Impact of Pure Copper Powder Reuse on Surface Chemistry During Powder Ded Fusion - Electron Beam**

__Sofia Kazi__, Phillip Mahoney, Eduard Hryha

Submitted for Journal Publication

V. **The Impact of Oxidation during Curing of Binder Jetted 17-4 PH Stainless Steel on Powder Properties and Powder Surface Chemistry**

__Sofia Kazi__, Kai Zissel, Eduard Hryha

Submitted for Journal Publication

Contribution of appended papers

I, III, IV: The author planned and conducted the experiments in collaboration with co-authors. The author conducted the analysis of the experiments and wrote the paper in collaboration with the co-authors. The co-authors helped with sample collection, provided useful information concerning the processing of the powder samples.

II: The corresponding author planned the experiments with the collaboration of co-authors as an extension of paper I. The author did the surface analysis of the powder and contributed to writing of this part.

V: The author planned the experiments with the collaboration of co-author. The author conducted the surface analysis of the powder. The co-author, Kai Zissel, was responsible for printing parts and providing the powder samples, flowability, oxygen and nitrogen content measurements and provided insights concerning these experimental procedures and processing of powders. The author wrote the paper with the help of co-authors.

ABBREVIATIONS

17-4 PH	Stainless steel 17-4
AM	Additive Manufacturing
BJT	Binder Jetting
BSE	Backscattered Electrons
CAD	Computer Aided Design
HR-SEM	High Resolution Scanning Electron Microscopy
OFHC-Cu	Oxygen Free High Conductivity Copper
PBF	Powder Bed Fusion
PBF-EB	Powder Bed Fusion-Electron Beam
PBF-LB	Powder Bed Fusion-Laser Beam
RQ	Research Questions
SE	Secondary Electrons
SEM	Scanning Electron Microscopy
316L	Stainless Steel 316L
XPS	X-ray Photoelectron Spectroscopy

Table of Contents

1. Introduction 1
  1.1 Background 1
  1.2 Research Objectives 2
2. Additive Manufacturing Technologies 3
  2.1 Powder Bed Fusion Techniques 3
    2.1.1 Powder Bed Fusion-Laser Beam (PBF-LB) 3
    2.1.2 Powder Bed Fusion-Electron Beam (PBF-EB) 4
  2.2 Binder Jetting (BJT) 6
3 Powders for AM 9
  3.1 Powder Manufacturing Methods 9
4 Powder Degradation in AM 11
  4.1 Powder Degradation in PBF-LB 11
  4.2 Powder Degradation in PBF-EB 13
  4.3 Powder Degradation in BJT 13
5 Materials and Methods 15
  5.1 Materials and Processing 15
    5.1.1 316L for PBF-LB 15
    5.1.2 Pure copper for PBF-EB 15
    5.1.3 17-4 PH for BJT 16
  5.2 Experimental Techniques 17
    5.2.1 Scanning Electron Microscopy (SEM) 17
    5.2.2 Surface Chemical Analysis 17
    5.2.3 Revolution Powder Analysis (RPA) 19
6 Summary of Appended Papers 21
7 Conclusions 27
8. Future Work 29
Acknowledgements 31
References 33

1. Introduction

1.1 Background

Additive Manufacturing (AM), also known as 3D printing, has been proposed as the latest solution to many limitations of traditional manufacturing technologies. The fundamental is the layer-by-layer deposition of material for fabrication of components, as opposed to the removal of material applied to subtractive manufacturing. It is this addition of material that promotes the cost-effectiveness of the technology and efficiency at mass production. Originally, AM was employed for rapid prototype fabrication as a cost-saving step in the manufacturing chain [1]. New advancements in the latest years in AM technology have rendered it a potential candidate for large scale manufacturing. With the assistance of a three-dimensional computer aided design (3D CAD) model, near-net-shape complex structures can be made in a shortened amount of time with increased material utilization [2].

Metal-based powder bed fusion techniques comprise only a branch of AM technologies. Here, a range of applications in the biomedical and aerospace fields benefit from techniques like powder bed fusion-laser-beam (PBF-LB) and powder bed fusion-electron-beam (PBF-EB). Fabrication of biocompatible Ti-based implants [3], Cu-based components for electrical and thermal applications [4], superalloy products for aerospace and energy are some of the few ways in which PBF-LB and PBF-EB have amassed attention due to design flexibility. Although not in the category of PBF techniques where the powder is physically melted during the printing process, metal binder jetting (M-BJT) is a sinter-based powder bed AM technology that utilizes a metal powder bed with the necessary deposition of liquid binder to produce smaller components compared to PBF-EB and PBF-LB, with higher productivity rates and surface finish.

As the feedstock material for the aforementioned techniques is powder, special interest has been expressed to study powder properties to ensure optimal processing and final part quality. A narrow particle size distribution can facilitate adequate powder bed packing, while powder morphology can ensure good flowability for layer deposition [5]. A controlled chemical composition of the powder with low oxygen content and absence of impurities is needed to ensure the desired mechanical properties of the printed component. Careful adjustment of these powder properties to accommodate the AM industry has made powder manufacturing one of the leading costs in AM [6].

Compared to the dynamic properties of powders, little attention has been paid to the effect of the printing processes on powder surface chemistry and how surface chemistry changes influence the final part quality. During powder bed fusion processing, the powder particles interact with the energy source, generating what is called “spatter”, highly oxidized particles that can end up on the powder bed and powder feedstock [7] and in subsequent prints can be melted as part of the printed components, introducing more oxides in the microstructure. Most of the spatter lands on the powder bed, leading to powder degradation over time by accumulating in the feedstock powder and resulting in its disqualification. Another example is the high temperatures of the powder bed in the PBF-EB process, which combined with the partial pressure of oxygen leads to oxidation of particles and hence powder degradation. In BJT, the powder is not heated during printing but humidified and later subjected to high temperatures during the “curing” in oxidizing atmosphere. This, coupled with the finer particle size, a characteristic of BJT powders and their higher surface area to volume ratio, results in higher levels of oxygen on the surface. Since a great cost in AM is the powder feedstock, more focused research is necessary to identify the degradation mechanisms of powder in AM processes upon reuse. This thesis aims to study the degradation mechanisms that powder is subjected to upon AM reuse with employment of surface characterization.

1.2 Research Objectives

The aim of this thesis is to understand the impact of AM technologies on powder degradation. So far, three compositions in three techniques have been examined, 316L in PBF-LB, 17-4 PH in BJT and pure Copper in PBF-EB. The objectives can be summarized below into the following research questions (RQ):

RQ1: What are the changes in powder surface chemistry in powder bed metal additive manufacturing depending on material and AM technology?

RQ2: What is the impact of powder recycling on powder properties in powder bed fusion?

2. Additive Manufacturing Technologies

Additive manufacturing encompasses a range of technologies that build 3D objects by adding material, such as polymers, metals, ceramics, or composites, in a layer-by-layer fashion, guided by computer-aided design (CAD) models [8]. This layer-by-layer approach enables the creation of intricate geometries and complex structures that were previously unattainable with traditional subtractive manufacturing technologies. Depending on the AM technology used, there is a possibility to adjust parameters such as laser power, layer thickness, build direction, support structures, cooling channels, etc.

Powder bed fusion (PBF) techniques alongside binder jetting (BJT) consist two of the most well-known and advantageous AM technologies to date. PBF techniques dominate the AM field currently, with the employment of an energy source, laser (PBF-LB) or electron beam (PBF-EB), and the local melting of a powder bed. In BJT, a powder bed is also an integral part of the process, with the powder particles of each layer being joined together with the aid of a binder. During subsequent steps, the binder is removed and the components are sintered to obtain the final density. This thesis will focus on the lifecycle and degradation of powders in PBF-LB, PBF-EB and BJT. The sections below offer an overview of these techniques.

2.1 Powder Bed Fusion Techniques

2.1.1 Powder Bed Fusion-Laser Beam (PBF-LB)

As the name suggests, in PBF-LB a focused laser beam is responsible for locally melting and fusing powder particles. It is considered one of the most versatile AM techniques given the plethora of alloy compositions that can be processed with it. A wide range of metal powders can be processed, including steels, Al-based alloys, Ti-based alloys, Ni-based superalloys and CoCr alloys, to mention some. The advantage of the technique lies in the fabrication of complex geometries with internal cooling channels, aiming to facilitate the circulation of cooling mediums. The printing process is carried out in an inert atmosphere with approximately 1000 ppm residual oxygen and the processing gas is usually argon or nitrogen. These conditions limit powder oxidation that is often caused by the reactivity of metal powders at elevated temperatures. Further explanation of powder oxidation and its mechanisms will be provided in a later chapter, but one of its side effects is the formation of non-metallic defects in printed parts that will compromise their properties.

Support structures are a habitual necessity in PBF-LB, type and density of which are dependent on the design complexity and build orientation of the printed part. Their presence also helps with dissipation of heat and thermal stresses due to high temperatures and rapid cooling cycles [9]. They also anchor the parts to the powder bed, thus limiting the possibility of distortions caused by these internal stresses and they prevent overhang features from collapsing since the powder bed provides minimal support. Their presence is also associated with increased time and cost since additional post processing time is also required for their removal and more powder is consumed overall.

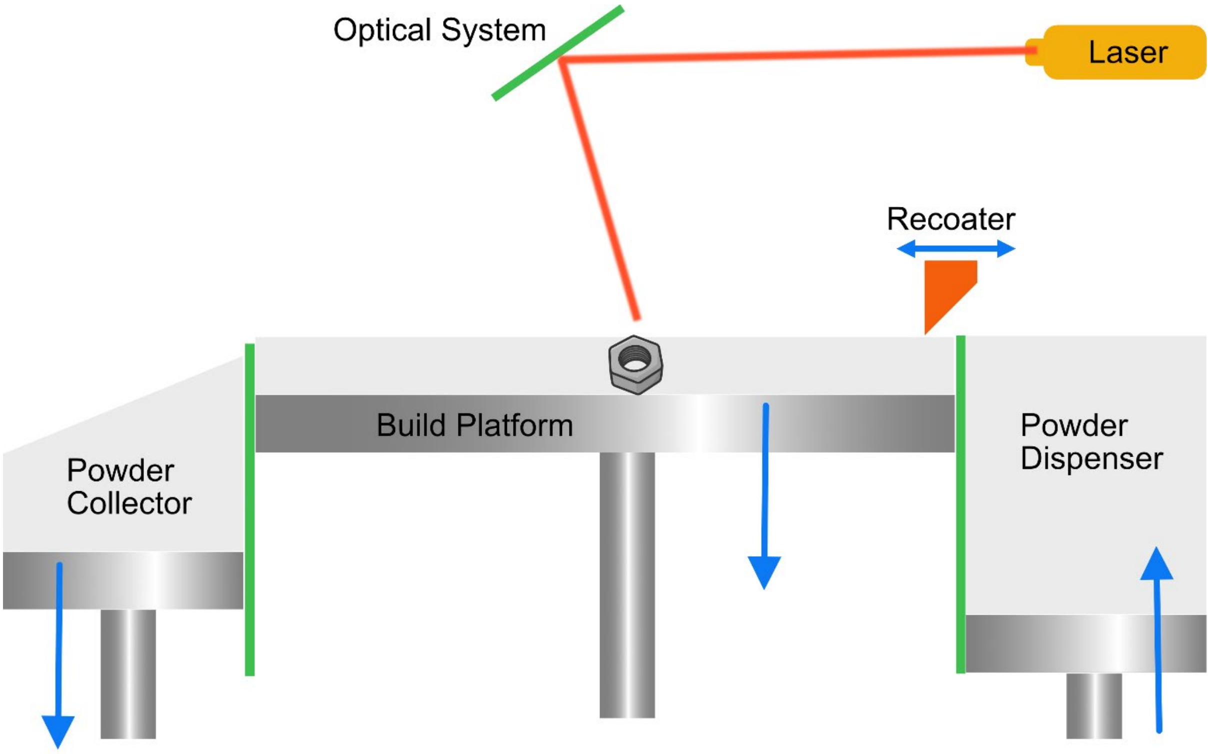

Figure 1: Schematic illustration of PBF-LB process. Redrawn from [10].

2.1.2 Powder Bed Fusion-Electron Beam (PBF-EB)

PBF-EB is an AM technique that selectively melts and fuses particles of a powder bed by utilizing a high-energy focused electron beam. Electromagnetic lenses help to control the beam position and intensity [11]. Conductive materials are required for this technique. A paramount necessity in this technique is a high vacuum environment. Without it, the electron beam would scatter, leading to decreased focus and precision. Another issue is the so called "smoking effect", where the interaction of the electron beam with metal particles causes electrostatic charging and powder ejection [12]. Conductivity is important since electrostatic charging can be more severe in less conductive materials, whereas conductive materials allow the dissipation of these charges [13]. The high energy emitted from the electron beam creates elevated temperatures in the chamber that would lead to increased oxidation of the powder in the absence of a vacuum environment.

To combat these issues, a high-vacuum environment is established before the printing begins, accompanied by a preheating step, to improve the conductivity of the powder bed. This step not only helps to mitigate the smoking effect but also helps the beam to reach the powder bed more efficiently [14], rendering the process more stable. Combined with conductive materials, preheating further increases conductivity, reducing thermal stresses and minimizing cracking or distortion. Preheating offers one more advantage, which is related to material consumption. Since the powder is sintered during the preheating step, it can act as a support for the complex geometries being printed, hence limiting the need to print support structures with the components, saving time, decreasing cost and powder usage.

Due to the high temperature developed during the printing process, cooling down of the chamber is necessary to avoid oxidation of the unused powder when in contact with air again. When the parts are removed from the chamber, they are surrounded by a “sinter cake”, created by the preheating step. A blasting procedure in air follows to break the sinter cake and remove the particles pre-sintered around the component. The particles are essentially used as the blasting medium to recover powder from sintering cake. Although PBF-EB necessitates the use of high vacuum accompanied by increased temperatures and powder bed pre-sintering for manufacturing of dense components with low thermal stresses, a major consequence becomes powder degradation.

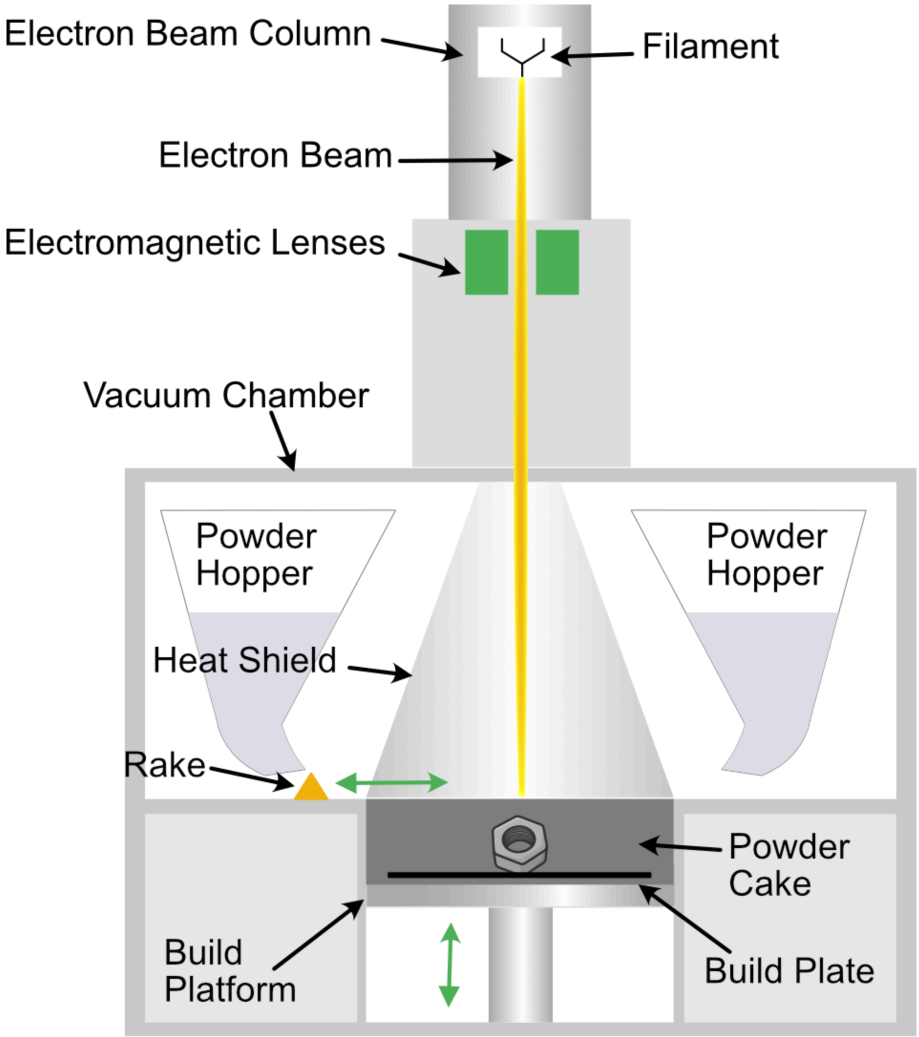

Figure 2: Schematic illustration of PBF-EB process.

2.2 Binder Jetting (BJT)

BJT entails a number of steps to attain the final components with the printing process being the first. A powder layer is spread with a roller blade and the particles are joined with the help of liquid binder droplets being deposited through a nozzle. This procedure continues iteratively until all the layers of the component are built. Here, the position where the binder is jetted creates the cross section of the component for each layer. Subsequent steps include curing, depowdering, debinding and sintering.

Printing, curing and depowdering are considered stages of the “green part” manufacturing. Green parts typically have green densities of ~50-60 % relative to the bulk material [15]. After printing, the powder bed containing the green parts is removed and curing at 80-250 °C takes place to harden the binder and evaporate residual water and solvents. Depowdering follows, where any loose powder of the powder bed is removed from the green parts that are a combination of hardened binder and metal powder. The thermal treatments of the green parts include debinding and sintering. During debinding, the parts are placed in a furnace and heated up to 600 ºC in order to remove the binder. In the last stage, the parts are sintered to achieve the final density. Sintering involves the bonding of metallic particles by atomic diffusion leading to formation of mechanical bonds that gradually increase the density of the material. Shrinkage also occurs due to bulk transport mechanisms involved in sintering [16].

The printing process itself is performed at ambient temperatures but the curing step where the loose powder is heated with the green parts renders the powder susceptible to oxidation since it is conducted in air.

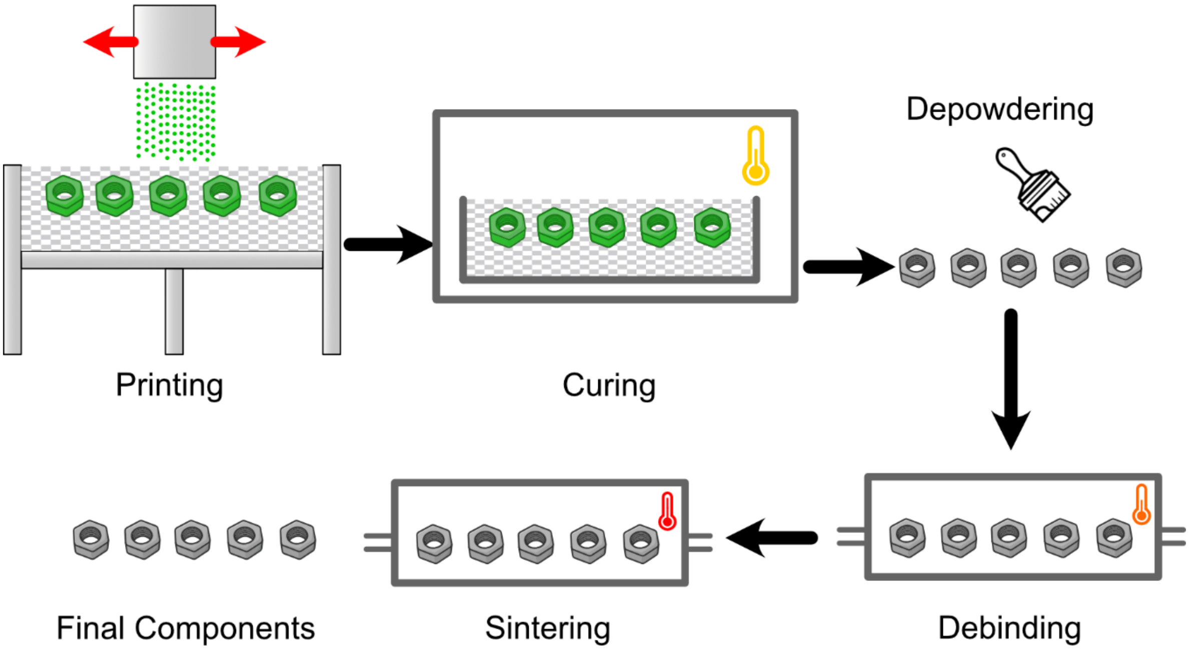

Figure 3: Schematic illustration of BJT printing process and subsequent steps until the final part retrieval.

3 Powders for AM

3.1 Powder Manufacturing Methods

With powder metallurgy being a prominent field, several fabrication routes exist currently that allow the production of metal powder from bulk material. Powders used in AM have to fulfill requirements regarding PSD, shape, morphology, surface chemistry and rheology to achieve processability in 3D-printing. Due to these prerequisites, atomization, the method of obtaining spherical-shaped metal powders by dispersion of melts [17], has emerged as the leading technology for powder production in AM. The most common atomization techniques used by industries today include inert gas atomization (GA), electrode induction gas atomization (EIGA), plasma atomization (PA) and vacuum induction inert gas atomization (VIGA).

Inert gas atomization is commonly used in industry because it allows the production of many alloy compositions. An inert gas is used, usually nitrogen or argon, responsible for breaking the liquid stream into droplets. The droplets then tend to solidify into near-spherical metal particles before they reach the bottom of the chamber and the range of their size can be monitored by the melt temperature, the volume and pressure of the gas and the nozzle orifice opening [18]. The Fe-based and Ni-based alloys are the usual candidates. An issue can be the susceptibility of the material to oxidation, in which case the metal is melted in a vacuum chamber through means of induction melting, and hence the process is called vacuum induction inert gas atomization (VIGA) [19]. Considering highly reactive metals like Ti-based alloys, VIGA's use of a crucible to contain the molten metal during heating presents a potential source of contamination. In such instances, EIGA offers a more advantageous approach. It involves melting a rod-shaped metal electrode through a crucible-free induction heating method, followed by the free-fall atomization of the molten metal using a high-velocity, high-pressure inert gas stream. This non-contact induction melting significantly reduces the risk of process-induced metallic impurities, enabling the production of high purity powders. Plasma atomization (PA) is another crucible-free atomization technique where a pre-alloyed wire is heated up to 10 000 K by plasma torches. This molten metal is then atomized into fine droplets using a high-velocity inert gas stream. Like in EIGA, the rapid solidification of these droplets results in highly spherical powder with high purity.

4 Powder Degradation in AM

As stated above, powders used for AM technologies must meet certain specifications regarding size, morphology, chemistry etc. The size, shape and morphology of particles has an effect on powder dynamic properties, i.e. rheology, which determines the spreadability of powder in a layer-like manner and the packing of said layer. The AM technologies discussed in Chapter 2 rely on spreadability and layer packing. Chemistry also determines the processability of powders in AM. It can refer to either bulk chemistry (composition) or surface chemistry, both of which can be impacted by the atomization process or during reuse in AM. Any changes in powder chemistry can lead to changes in the properties of the final parts.

One of the significant advantages in powder-based AM that has earned the technology distinction from other fabrication routes is the reusability of feedstock powder material. The possibility of reusing the same powder batch that has not been melted and solidified into bulk components for multiple consecutive prints enables the sustainability of the process. Nevertheless, the processing conditions of different AM techniques can have a negative impact on the powder properties with reuse and lead to defects and decreased performance in the printed parts.

Beyond moisture, the powder can also pick up impurities like oxygen, nitrogen, carbon, and hydrogen from the surrounding atmosphere or the process gases used in the printing machine, further contributing to its degradation over time. Maintaining a controlled environment throughout the entire manufacturing process is paramount to prevent powder contamination.

4.1 Powder Degradation in PBF-LB

The primary causes of powder degradation in AM include oxidation, changes in particle size distribution and morphology and contamination. Particularly in PBF-LB, the printing is carried out in an inert atmosphere aided by nitrogen or argon flow. Even under this controlled atmosphere, trace amounts of residual oxygen or moisture coupled with elevated temperatures can lead to oxidation due to the powder’s fine particle size and large surface area, rendering them highly susceptible to reacting with oxygen present in the atmosphere. Certain elements commonly found in PBF-LB materials, such as aluminum, titanium, chromium, and magnesium, have a strong affinity for oxygen and readily form oxide products on the powder surface, the composition and size of which are determined by powder chemistry and processing conditions. Furthermore, the practice of preheating the build platform, while beneficial for reducing thermal stresses and improving part quality in some cases, can also accelerate the oxidation process by maintaining the powder at elevated temperatures for extended durations.

Another aspect of PBF-LB needing consideration is the intricate interaction of the laser beam with the powder bed. The heat generated by the laser melts the powder particles, creating a molten pool. The intense heat causes some of the molten metal to vaporize, turning into gas. This gas expands rapidly, pushing outward with a force called recoil pressure. This low-pressure zone acts like a vacuum, pulling on both the gas and the molten metal, leading to the formation of hot and cold spatter [20], [21], [22]. The amount and characteristics of spatter are influenced by various factors, including laser power density, scanning speed, the type of alloy being processed, and the flow of the inert gas within the build chamber. One of these factors discussed in literature is the effect of processing gas in the printing chamber, where the use of helium was proven to lower the amount of generated spatter particles by 30% compared to the use of pure argon [23], and had a positive impact on the surface finish of the samples due to this reduction [24]. Previous studies on PBF-LB processing of Hastelloy X have shown that an increase in layer thickness during the printing process can result in a higher amount of generated hot spatter [25]. Chen et al. showed that complex geometrical features like overhang structures produce local overheating and can generate more spatter due to their larger surface-to-volume ratio [26]. These spatter particles often exhibit non-spherical shapes and a wider range of sizes compared to the original powder. When these spatter particles re-deposit onto the powder bed and printed components, they can lead to various defects in the final part, such as surface irregularities and embedded unmelted particles, ultimately increasing porosity. Longterm reuse of AlSi10Mg powder in PBF-LB, resulted in reduced tensile and hardness properties attributable to the increased size of gas pores in the printed specimen [27], where accumulation of spatter and increase in oxidation caused the increased porosity in the parts [28].

Another morphological change that can occur is agglomeration, where powder particles clump together. This can be caused by electrostatic forces between fine particles, the absorption of moisture from the environment and partial sintering due to residual heat in the powder bed. Agglomerated powder tends to exhibit poor flowability and spreadability, making it difficult for the recoating system to create a uniform powder layer, which can lead to lack of fusion defects in the printed part.

4.2 Powder Degradation in PBF-EB

While PBF-EB is conducted under high vacuum that minimizes the possibility of powder oxidation, other aspects of the process may lead to powder degradation. In chapter 2.1.2, the preheating step was mentioned as an important mechanism to improve the conductivity of the powder bed and aid the electron beam to effectively reach and melt the powder bed. The high temperatures developed during sintering can lead to powder oxidation, especially for alloys containing elements with high affinity for oxygen, even at low partial pressures. Gruber et al. showed that Alloy 718 powder underwent severe oxidation throughout reuse, with Al-based oxide nano-particulates dominating the surface of the powder particles [29] that end up in the fabricated samples as inclusions [30]. Sun et al. reported a 35% increase in oxygen content of TiAl6V4 powder after 30 printing cycles in PBF-EB, with more irregular morphology after reuse (possibly a result of blasting) and narrower PSD, likely due to sieving [31]. TEM on the powders failed to detect a change in oxide layer thickness but the microstructure of powders changed.

Another issue arising from the combination of high-vacuum and elevated temperatures under which printing in PBF-EB is conducted (650-1000 ºC), is the sublimation of certain elements. This phenomenon where elements transition from solid to gas phase in absence of the liquid phase, is called metallization and can alter the composition of the fabricated parts due to certain volatile elements sublimating from the surface of the feedstock powder [32]. Al and Cr in Alloy 718 have been found to vaporize and form metal condensates that get deposited on the heat shields of the machine [33]. Al has also been shown to reduce in TiAl6V4 with reuse but remained within an acceptable range [34]. The high temperatures developing during printing pose a limit on the monitoring devices that could potentially be employed to analyze metallization.

4.3 Powder Degradation in BJT

Opposing the PBF trend of melting and solidifying powder particles during printing, the printing process in BJT includes the bonding of particles with the aid of a binder at room temperatures, thus mitigating the possibility of powder oxidation [35]. This is said to enhance the reusability of powders, thus rendering BJT a sustainable process.

The PSD of powder used in BJT is usually within the 5-20 μm range to achieve better sinterability. Such small particles tend to be more cohesive and flow in agglomerates. To combat this, conditioning of the powder is usually applied before printing, meaning oxidation of the powder to improve flowability. The optimal conditioning strategy was tested for TiAl6V4 [36], as well as optimal drying conditions where it was shown that drying in ambient air for longer periods had a positive effect on flowability and reducing the water content of the powder. Later, it was shown that reuse of TiAl6V4 led to a significant increase in oxygen and nitrogen content after the first use but subsequent reuse of the powder had a less significant effect on the oxygen and nitrogen content of the powders, while changes in the cohesion of the powder were difficult to observe [37]. Zissel et al. observed that reuse of 17-4 PH powder resulted in an uptake in oxygen content after initial printing but the increase was less severe for the following printing cycles. The rise in oxygen content was attributed to the curing stage that was carried out in air [38]. A study on the reuse of 316L found a small increase in oxygen and an increase in flowability due to coarsening of the PSD, due to loss of fine particles [39].

5 Materials and Methods

In this section, the materials used in this study alongside the characterization techniques used will be presented.

5.1 Materials and Processing

5.1.1 316L for PBF-LB

Stainless steel 316L is one of the most commonly used materials in PBF-LB due to its excellent corrosion resistance and strength properties. In this study, the 316L powder was produced by Oerlikon Metco with inert gas atomization, possessing a PSD of D_{10} = 19 µm, D_{50} = 30 µm, D_{90} = 46 µm. The powder was processed in a metal powder bed fusion machine Trumpf TruPrint 5000 at Alfa Laval. In Paper I, the powder samples used for investigation consist of virgin powder that was loaded into the machine before the first print job and reused with no mixing. Paper II included reused powder of a different batch but with the same composition as well as atomized powder produced from AM scrap and disqualified 316L powder as an extension of Paper I. Table 1 summarizes the collected samples used in this study.

Table 1: The annotation of the samples based on reuse.

Sample name	No. of print jobs	Printed Volume	Exposure Duration	Total Exposure Duration
Virgin	-	-	-	-
P5	5	496 cm^3	10.5 h	56 h
P7	7	805 cm^3	20 h	97 h
P9	9	650 cm^3	16 h	133 h
P11	11	223 cm^3	4.5 h	140 h
Atomized	-	-	-	-

5.1.2 Pure copper for PBF-EB

Oxygen-free high conductivity (OFH-Cu) copper powder produced by ECKART GmbH using inert gas atomization was used in PBF-EB, with a PSD of D_{10} = 50.5 µm, D_{50} = 72 µm and D_{90} = 98.6 µm.

The copper powder was processed using an ARCAM EBM Q10 metal powder bed fusion machine equipped with a Spectra EBU version 1.2. The preparation of the machine included evacuation of the chamber to high vacuum to avoid evaporation of material before being filled with helium gas. The samples used in Paper III included virgin powder retrieved from the hoppers (sample marked as V/hoppers) and as a result exposed to the chamber conditions during printing, and reused powders retrieved after printing and blasting. Additionally, a powder reused 6 times again (P6/b) was used for printing under altered conditions, using helium gas of lower purity. In paper IV, as-atomized virgin powder was used for the study without being put in the machine and the reused powders from Paper III, as a more in-depth work on the effect of reuse and processing conditions on pure copper.

Table 2: The annotation of the samples based on the amount of print jobs.

Sample name	**No. of print jobs**
Virgin	-
V/hoppers	-
P6	6
P6/b	6
P8	8

5.1.3 17-4 PH for BJT

N_2-atomized pre-alloyed 17-4 PH stainless steel powder (Desktop Metal Inc., USA) was studied in BJT with a PSD of D_{10} = 6.5 µm, D_{50} = 14.3 µm, D_{90} = 26 µm. A Production System™ P-1 (Desktop Metal Inc., USA) was employed for BJT printing. A water-based binder (SPJ-04, Desktop Metal Inc., USA) was used for printing. Virgin powder was loaded into the printer and reused for five build jobs, followed by curing the five obtained build boxes simultaneously.

Curing took place in an air-convection furnace (TR 120 LS, Nabertherm GmbH, Germany), with a heating rate of 1.5 °C/min to a maximum temperature of 200 °C and 4 h dwell time. After air-cooling and depowdering the powder was reused for 5 consecutive build jobs. This was repeated for 20 printing jobs and four curing processes in total.

The powders used for investigation in BJT consist of unconditioned powder, virgin powder that was loaded into the machine before the first print job and sieved powders collected from depowdering after each curing cycle. Table 3 summarizes the collected samples used in this work, where C1-4 described the amount of curing cycles the powder was subjected to.

Table 3: The annotation of the samples based on the amount of print jobs in machine.

Sample name	Total no. of print jobs	No. of curing processes
Unconditioned	-	-
Virgin	-	-
C1	5	1
C2	10	2
C3	15	3
C4	20	4

5.2 Experimental Techniques

5.2.1 Scanning Electron Microscopy (SEM)

A Leo Gemini 450 SEM (Zeiss GmbH, Germany) was employed to study the powder morphology. Due to the electron beam's significantly shorter wavelength compared to visible light, SEM imaging provides a much higher resolution than optical microscopy. This is achieved by scanning the sample with a focused electron beam, converting the detected signals to grayscale images [40]. The electron beam is generated by a field emission gun, which is directed onto the sample via electromagnetic lenses. The incident electron beam energy, typically ranging from 3 to 30 kV, influences the interaction volume within the sample, which also depends on material type and incidence angle. These signals result from interactions between the electron beam and the sample's electrons, categorized as inelastic and elastic interactions. Inelastic interactions produce low-energy secondary electrons (SEs), which are emitted near the sample surface. Detecting SEs allows for detailed analysis of the sample's surface topography and morphology due to their curved path to the collector [41]. Elastic interactions generate backscattered electrons (BSE’s), which originate from a larger interaction volume compared to SEs. BSE intensity is proportional to the atomic number of the elements present, enabling chemical contrast imaging where heavier elements appear brighter. Furthermore, the relaxation of ionized atoms results in the emission of X-rays, which are analyzed using energy dispersive spectroscopy (EDS) to determine the elemental composition of the sample.

5.2.2 Surface Chemical Analysis

X-ray photoelectron spectroscopy (XPS) is a highly effective technique for analyzing the surface chemistry, oxidation states, oxide layer thickness, and oxide types of materials with exceptional surface sensitivity (approximately 10 nm). The XPS systems consist of an X-ray source, and analyzer and a detector, all secured in an ultra-high vacuum (UHV) environment (10^{-9} – 10^{-10} mbar). In XPS, X-rays are employed to bombard the surface of the sample and photoelectrons are emitted, the kinetic energy of which is analyzed [42]. The kinetic energy (KE) is later converted to binding energy (BE) following the mathematical equation:

$$BE = h\upsilon - KE - W \tag{1}$$

This equation states that the energy of the X-ray ($h\upsilon$) is the total of the binding energy (BE) of the electron, the kinetic energy (KE) of the emitted electron and the spectrometer work function (W), a constant value. To ensure consistent data, the resulting polychromatic X-rays are passed through a monochromator, selecting a single wavelength for analysis. These monochromatic X-rays interact with the sample surface, ejecting core-level electrons (photoelectrons).

The first step in XPS is to determine the present elements on the surface of the sample before trying to decipher their chemical state. The first step is done by conducting survey spectra over a large energy range (0-1416 eV) using either monochromatic Al K□ or non-monochromatic Mg K□ source. For chemical analysis, narrow scan spectra are captured by narrowing the binding energy range. The chemical state can also be analyzed across different depths by employing the depth profiling function, where ionized inert gas beam scanned over the sample etches the surface.

In this thesis, XPS analysis is conducted by using PHI 5000 (Physical Electronics, MN, USA) equipped with monochromated Al Kα source (1486.6 eV). The 316L powders were lightly pressed on pure Al-plates, whereas the Cu-powder and 17-4 PH were mounted on carbon tape due to their softness and small PSD, respectively. The commonly used pass energies for survey spectra were 224 eV and for narrow scans 26 eV. During depth profiling, Ar$^+$ ion etching was conducted, where the etch rate was calibrated on a flat oxidized tantalum foil with known Ta_2O_5 oxide thickness. The depth profiling was conducted over an area of 2 mm x 2 mm down to an etch depth of 100 nm. Hence, all the etch depths mentioned are in Ta_2O_5 units. All the data analysis was carried out in the PHI MultiPak.

5.2.3 Revolution Powder Analysis (RPA)

One key point of powder processing in powder-based additive manufacturing is the feedstock powder’s ability to flow and create uniform layers with high packing ability [43]. To test the flow properties of powders for AM, a Revolution Powder Analyzer (Mercury Scientific Inc., USA) was employed. The RPA works on a rather simple principle. It entails a setup with a transparent drum filled with material, which rotates according to user-defined settings. On the other side of the setup, a camera captures the movement of the material, which is illuminated by a light source. The camera records the surface area of the moving powder, and this data is subsequently processed using specialized image analysis software.

For each test, a consistent powder volume of 30 ml or 100 ml is carefully poured into the drum without compaction. Different measurements can be used to analyze a number of flow metrics for the powders and correlate them to the powder’s ability to be processed in AM. The simplest test, a flowability test, uses constant rotating speeds to capture the movement of powder for a specific time interval or a set number of avalanches in the drum. The powder can also be tested across a number of rotating speeds (multiflow test) or even undergo consecutive vibrations to establish its packing behavior by measuring its apparent and tap density (packing test).

For the study presented in this thesis, the rheological tests were performed in ambient conditions. To explore the multi-flow behavior, experiments were performed by systematically varying the drum's rotation speed from 1 to 70 RPM, with incremental steps of 2 RPM. At each specific rotation speed within this range, 75 individual powder avalanches were recorded and analyzed.

6 Summary of Appended Papers

This chapter summarizes the key research findings and provides an overview of the appended papers. The thesis addresses two main research questions. The first research question, RQ1, explored in Papers I-V, focuses on powder degradation and changes in surface chemistry based on composition and AM technology. The second question, RQ2, concerning the effect of powder recycling is explored in Paper II.

Papers I and II – Study on 316L for PBF-LB

In Paper I, 316L virgin powder was initially processed in the PBF-LB machine, sieved and reused for over 140 hours of total exposure time. The same batch of powder was used for all subsequent prints and no mixing of powder batches occurred.

Evaluation of the morphology of virgin powder revealed particles with spherical morphology and rather pure surface, see Figure 4(a, b), with some seldom presence of a bit more oxidized particles. Printing using PBF-LB technique led to generation of spatter particles that could be seen due to the evident oxidation of particles, as seen in Figure 4(c, d).

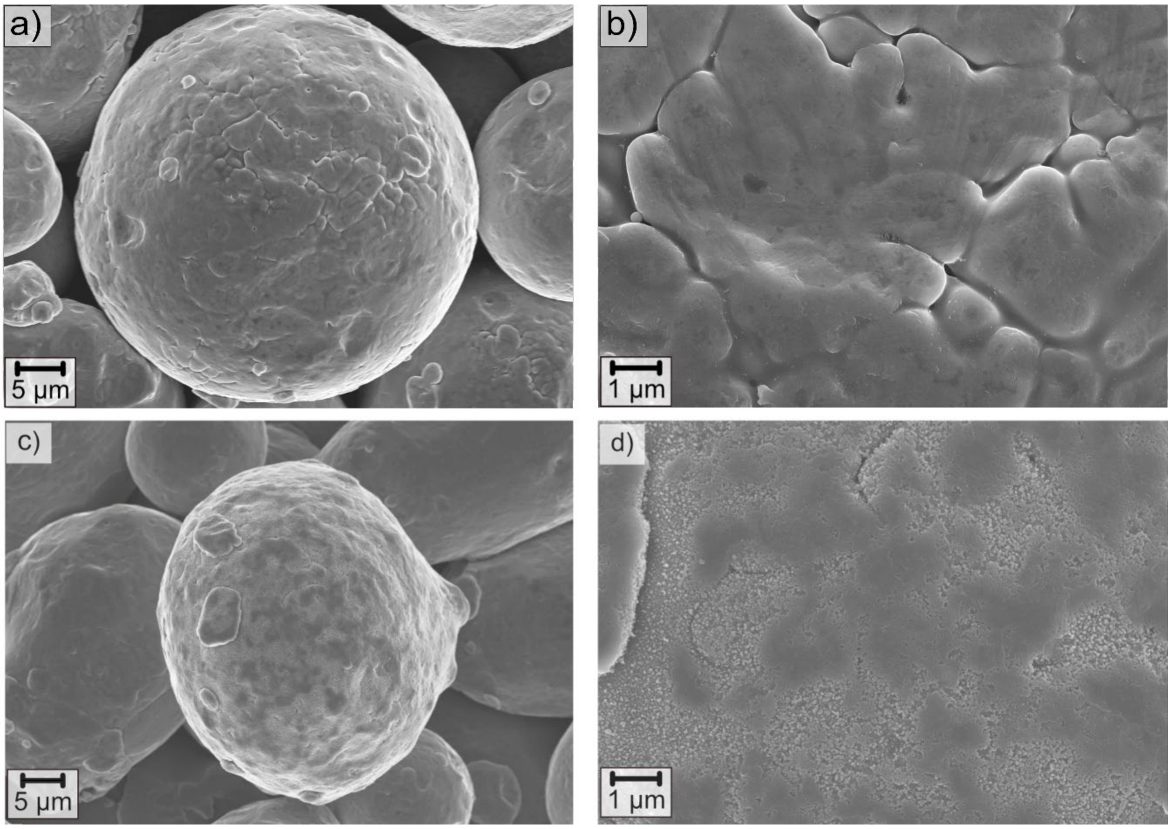

Figure 4: SEM micrographs of 316L powder virgin particle at a) low and b) high magnification, and spatter particle from P5 at c) low and d) high magnification.

XPS depth profiling revealed the presence of Fe-based oxide layer (with some presence of Cr in the oxide layer as well), mainly Fe_2O_3, with Cr, Mn, and Si enrichments on the surface of the particles in the form of oxide nano-particulates in the virgin powder as well as the reused variants. Figure 5 showcases the progressive increase of the oxide layer thickness with reuse of the powder in the PBF-LB machine. The oxide layer thickness was calculated by using the model developed in previous XPS studies [44], [45]. Depth profiling in combination with this model revealed that the virgin sample had an average oxide layer thickness of ~4.8 nm and this increased up to ~8 nm for the P11 (most reused powder that was exposed for 140 h in total). These findings are most likely attributed to an increase of oxide nano-particulates on the surface of the powders particles as well as accumulation of spatter in the feedstock powders.

In Paper II, disqualified powder of 316L from PBF-LB printing and AM scrap components were atomized in nitrogen atmosphere. From the re-atomized powder, PSD of 15-45 μm (commonly used PSD for PBF-LB) was separated and the surface morphology and chemistry was studied. XPS measurements showed that the re-atomized powder had a smaller oxide layer thickness than the previously measured virgin powder, approximately 4 nm. In SEM, lower surface oxidation was also observed, and contrary to the virgin powder, no oxidized particles could be seen. It is assumed that the absence of oxidized particles in the re-atomized powder is a reason for the overall lower oxide layer thickness.

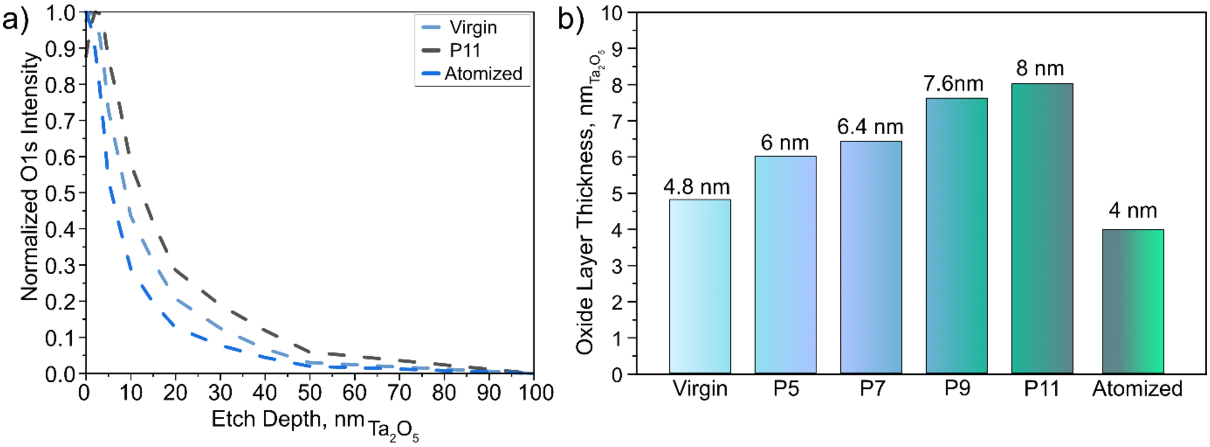

Figure 5: Normalized oxygen content from O1s narrow spectra of 316L samples plotted against etch depth.

Papers III and IV – Study on OFHC-Cu in PBF-EB

In Papers III and IV, the reusability of oxygen-free high conductivity (OFHC) copper powder was tested in PBF-EB machine. Virgin and reused powders were analyzed using XPS and SEM. The morphological observations in SEM showed that the oxide features covering the surface of the powder samples differed in morphology depending on the printing conditions, suggesting the presence of different types of surface oxides. The samples were thus analyzed in XPS, and peak fitting showed that the oxide from thin oxide layer primary consisted of CuO with Cu_2O particulates alongside $Cu(OH)_2$. When the PBF-EB process was carried out under industrial standardized conditions followed by exposure to ambient conditions and/or blasting, XPS on the reused powders revealed the transformation of the dominant CuO to Cu_2O due to growth and accumulation of oxide nanoparticulates on the surface. The oxide layer thickness for the virgin powder where CuO was the dominant surface oxide, was calculated to be ~2.5 nm. The reused powders P6 an P8, where Cu_2O was the main surface oxide (in the form of oxide nano-particulates) had similar oxide layer thickness ~2.5-2.8 nm. Powder handling had a strong effect on powder surface oxide composition, with increasing fraction of CuO and especially copper hydroxide ($Cu(OH)_2$) observed from the XPS analysis when processed with lower purity purging He gas. In that case the oxide layer thickness increased severely to ~19 nm. Powder from the hoppers (V/hoppers), that was not pre-sintered but exposed to the elevated temperature and vacuum, also showed higher oxide layer thickness that the virgin one reaching ~9 nm, formed mainly by CuO and $Cu(OH)_2$. Hence, it can be concluded that copper powder is very sensitive to handling and PBF-EB processing but possesses excellent reusability when properly handled and processed in controlled environment.

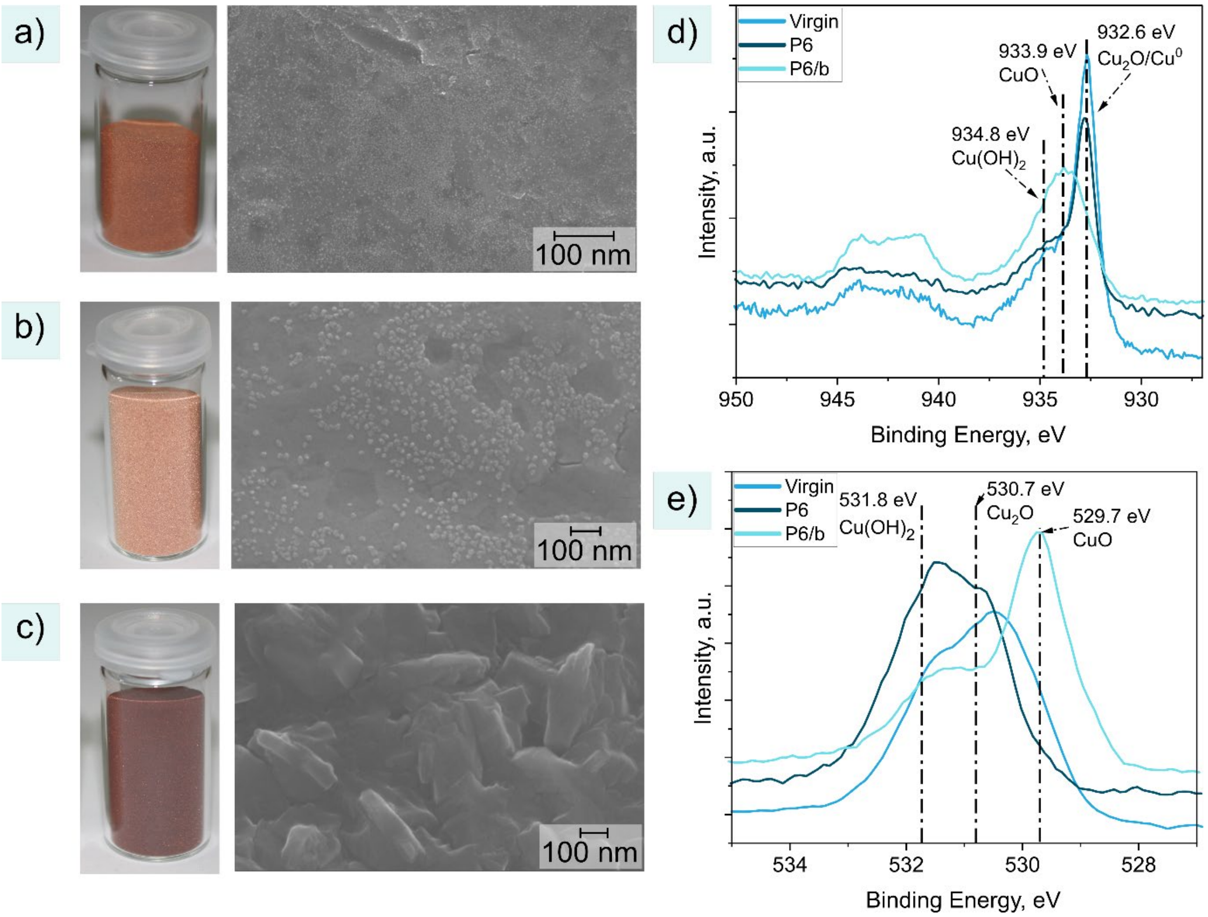

Figure 6: SEM micrographs of pure Cu samples in PBF-EB with pictures depicting the effect of processing on the colors of the sample powders. a) Virgin, b) P6 used, c) P6/b used. On the right, XPS narrow scans of virgin, x6 and x6/b samples at the as-received surface. d) Cu2p spectra and e) O1s spectra.

Paper V – Study of 17-4 PH in BJT

In Paper V, 17-4 PH powder was analyzed after subsequent curing cycles during BJT. Unconditioned and virgin powder was also sent from the manufacturer to assess the effect of conditioning on the surface chemistry of the powders and flowability. It was found that the highest oxygen pickup took place after conditioning of the powder, whereas curing after printing had a lower oxidizing effect, see Figure 7(a). Nitrogen content remained mostly constant for all the samples. Surface analysis by means of XPS revealed the progressive increase in the oxide layer thickness on the surface of the particles, from ~4 nm for the unconditioned powder to ~7 nm for the virgin powder sample following similar trend as the oxygen content measurements. Curing of the powder after printing further increased the oxide layer thickness to ~9.5 nm for all the cured powders. Surface analysis thus confirmed that each curing cycle had less impact on the surface oxidation of the powders as four curing cycles resulted in an increase in oxygen content to approximately 1500 ppm from 1200 ppm in the virgin state

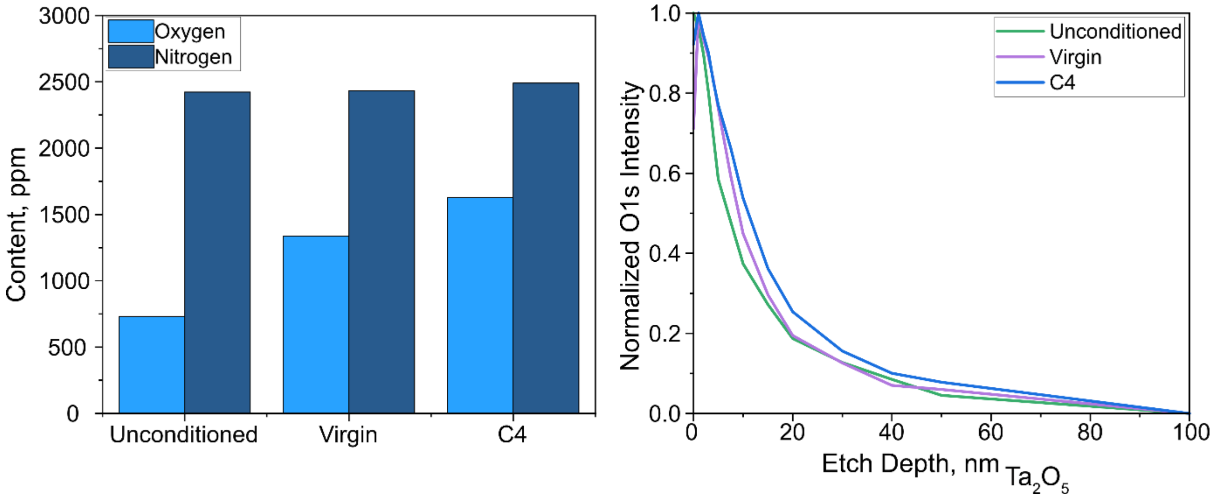

Figure 7: Oxygen and nitrogen content measurements (left) and normalized intensity of O1s spectra to etch depth (right) for unconditioned, virgin and C4 samples. The etch rates, therefore etch depths, were calibrated using Ta_2O_5 *foil of known thickness.*

The as-atomized unconditioned 17-4 PH powder was too cohesive and proved to flow in agglomerates rather than individual particles, even though it had a very low oxide layer thickness and low oxygen content. Conditioning of the powder, even though resulting in increase in oxygen content due to the oxidation, proved necessary to enhance the flowability and spreadability of the powder before printing, that affected the oxide layer thickness by an increase of ~3 nm and an uptake of ~600 ppm in overall oxygen content. This step reduced the inter-particle friction and lowered the Van der Waals forces between the particles, thus increasing flowability.

Flowability measurements reveal an increase in the flow behavior of powder samples with an increase in oxidation. Different flowability metrics that are plotted in Figure 8 showcase a positive effect of oxidation likely due to the decrease of the cohesion between powder particles.

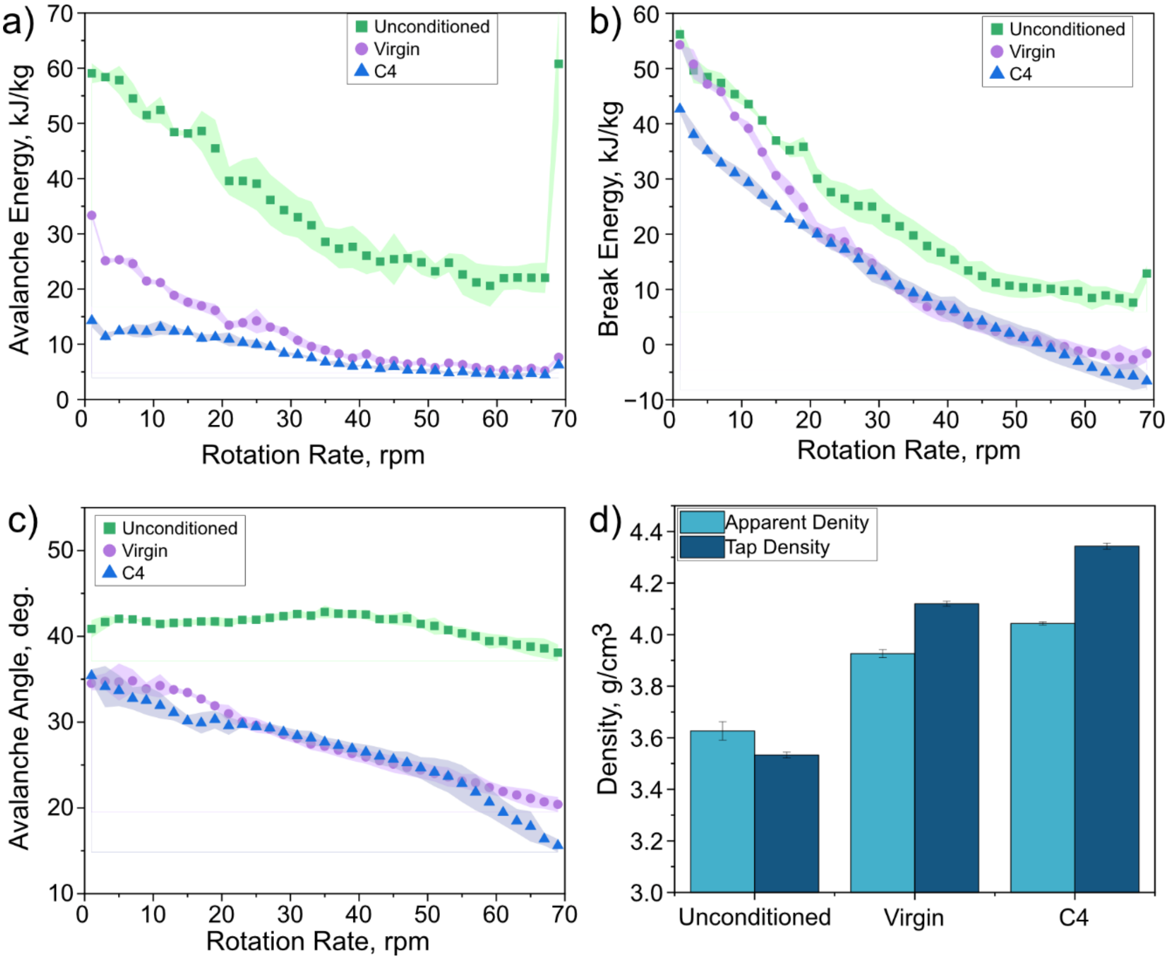

Figure 8: Rheological behavior of the unconditioned, virgin and C4 samples using the multiflow test in the range of 1-70 rpm. a) Avalanche energy, b) break energy, c) avalanche angle and d) tap and apparent density. Each powder was tested 3 times and the mean values with standard deviations have been plotted for each rotating speed and each packing measurement.

7 Conclusions

7.1 RQ1: What are the changes in powder surface chemistry in powder bed-based metal additive manufacturing depending on material and AM technology?

It was found that spatter formation in PBF-LB was a dominant degrading mechanism, with spatter particles ending up mixing in the feedstock powder and accumulation with reuse leading to an apparent increase in the oxide layer thickness. The virgin powder consisted of particles with dendritic structure with low number of particles appearing visually oxidized. In reused samples, spatter particles could be detected with their fraction increasing with reuse. The oxide layer thickness in the virgin powder in case of stainless steel 316L was calculated at ~4.8 nm and experienced a gradual increase with increasing reuse and was found to be ~8 nm for the most reused powder after exposure to a total of ~140 hours.

Degradation of OFHC-Cu powder in PBF-EB was connected to a transformation of CuO to Cu_2O during PBF-EB processing due to processing in vacuum at elevated temperatures. It was also shown that powder is very sensitive to oxygen partial pressure in the vacuum and powder handling. Oxide layer thickness was calculated at ~2.5-2.8 nm for virgin and reused powders. However, powder sampled from the hoppers, that was exposed to similar chamber conditions during printing, showed increased oxide layer thickness of ~9 nm, formed mainly by CuO and $Cu(OH)_2$, confirming oxidation under these conditions. Purging gas (He) with higher trace oxygen content led to increase in oxidation with dominant CuO and $Cu(OH)_2$, with a ~19 nm oxide layer causing process instability and powder disqualification.

The 17-4 PH powder experienced an increase in the Fe-based oxide layer thickness with curing. The surface of the particles was also enriched in oxide particulates rich in Cr, Mn, Si, Nb. Curing did not occur at such high temperatures to alter the surface chemistry in terms of surface oxide composition. The unconditioned 17-4 PH powder exhibited poor flowability due to its cohesive nature and tendency to agglomerate. A conditioning step resulted in an approximately 3 nm increase in the oxide layer thickness and a corresponding rise of around 600 ppm in the overall oxygen content. This controlled oxidation improved powder flowability. Similarly, multiple curing cycles of the powder also contributed to enhanced flowability and packing albeit with minor increase in the oxide layer thickness. These findings underscore the critical role of surface modification through controlled oxidation in tailoring the flow properties of metal powders for successful implementation in BJT processing.

7.2 RQ2: What is the impact of powder recycling on powder properties in powder bed fusion?

In 316L, the surface of particles in the virgin and reused powders was enriched with Cr, Mn and Si in oxidized state, content of which significantly increase with the powder reuse, indicating high temperature oxidation due to processing. Reuse in PBF-LB led to gradual increase in oxide layer thickness that reached approximately 8 nm in the most reused sample. It was shown that it is possible to reverse the surface oxidation and degradation of powders by re-atomizing disqualified powder and AM failed components. The re-atomized powder had an oxide layer thickness of ~4 nm, similar to the virgin powder (~4.5 nm) while retaining almost the same powder properties. Lower content of Si was found to be present in re-atomized powder compared to the virgin and reused powder before atomization.

8. Future Work

In Paper I, the oxide layer thickness of the 316L powder was increased with reuse in PBF-LB. Spatter accumulation was also detected and its fraction in the powder batch increased with reuse. In Paper II, recycling of 316L proved to successfully lower the surface oxide layer thickness. The next step will be to compare the dynamic properties of virgin, reused and atomized powders as well as examine the impact of recycling on mechanical properties, as well as corrosion. Paper II established an atomization path for 316L failed components and reused powder, hence atomization of used powder and scrap will be part of the future studies to enhance sustainability in AM. Recycling of other materials in PBF-LB, such as Ni-base and Al-base alloys and the effect of recycling on material properties and performance will be part of future studies. It is of imperative importance not only to study the powder degradation and its effects on printed parts but also to establish a robust recycling path for the reused/disqualified powders and printed components.

In Papers III and IV, reuse of OFHC-Cu powder in PBF-EB resulted in transformation of the dominant surface oxide from CuO to Cu_2O with presence of $Cu(OH)_2$. The purity of the processing He gas proved to be vital, as the use of low purity He led to increase of the oxide layer thickness to 19 nm approximately and disqualification of the powder. As copper is a material of great interest for its thermal and electrical conductivity, and it is known that impurities such as oxygen can have a negative impact on these properties, it is important to study the effect of powder reuse and increase of surface oxidation on the conductivity of printed parts.

In Paper V, consecutive curing cycles had little effect on the surface oxidation of 17-4 PH while the flowability showed positive changes. Further in-depth analysis using variety of surface and microscopy techniques should be done to provide insights into the effect of curing cycles on other materials containing elements with high oxygen affinity, for example, Ti-based, Ni-based and Al-based materials.

Acknowledgements

I would like to take this opportunity to thank both my supervisors Professor Eduard Hryha and Professor Yu Cao for giving me this opportunity and their constant support and interesting discussions. I would also like to thank my examiner Professor Lars Nyborg and my division head Professor Uta Klement for their support. I would like to acknowledge the Centre for Additive Manufacture Metal (CAM2) funded by Vinnova under which part of this thesis work has been carried out.

Special gratitude is owed to Dr. Eric Tam for teaching me the XPS technique, always answering my questions, putting up with my mistakes, fixing the XPS machine whenever I cause malfunctions to it and providing overall support and patiently allowing me to complain. I would also like to express my appreciation to Dr. Gowtham Soundarapandiyan for our collaboration and the insights he provides in our projects, Dr. Dmitri Riabov and Dr. Antonio Mulone for their assistance.

I would like to also thank my colleagues and friends at the Department of Industrial and Material Science and the friends I have made outside of the workplace that constantly let me nag. I am grateful to my officemate Dr. Valentina Matovic for always cheering me up.

I am grateful to Professor Sheng Guo for accepting me originally as a trainee in the department thus introducing me to AM and creating the opportunity for me to apply for the PhD position.

I would like to thank my family and friends at home for their love and support and always encouraging my ambitions.

Last but not least, research engineer Johnny Mikael Meant Hamnesjö Olausson Santos has been carrying me on his shoulders since my interview for the PhD position and this thesis work would have not been carried out without him, his never-ending help inside the lab, his support outside the workplace and his couch.

References

[1] M. Greul, T. Pintat, and M. Greulich, “Rapid prototyping of functional metallic parts,” *Comput Ind*, vol. 28, no. 1, pp. 23–28, Dec. 1995, doi: 10.1016/0166-3615(95)00028-5.

[2] M. Srivastava, S. Rathee, S. Maheshwari, and T. Kundra, *Additive Manufacturing: Fundamentals and Advancements*, 1st ed. CRC Press, 2019. doi: https://doi.org/10.1201/9781351049382.

[3] S. Singh and S. Ramakrishna, “Biomedical applications of additive manufacturing: Present and future,” *Curr Opin Biomed Eng*, vol. 2, pp. 105–115, Jun. 2017, doi: 10.1016/J.COBME.2017.05.006.

[4] S. J. Raab, R. Guschlbauer, M. A. Lodes, and C. Körner, “Thermal and Electrical Conductivity of 99.9% Pure Copper Processed via Selective Electron Beam Melting,” *Adv Eng Mater*, vol. 18, no. 9, pp. 1661–1666, Sep. 2016, doi: 10.1002/ADEM.201600078.

[5] S. E. Brika, M. Letenneur, C. A. Dion, and V. Brailovski, “Influence of particle morphology and size distribution on the powder flowability and laser powder bed fusion manufacturability of Ti-6Al-4V alloy,” *Addit Manuf*, vol. 31, p. 100929, Jan. 2020, doi: 10.1016/J.ADDMA.2019.100929.

[6] I. Campell, O. Diegel, J. Kowen, and T. Wohlers, “ Wohlers Report 2017: 3D Printing and Additive Manufacturing State of the Industry, Annual Worldwide Progress Report,” 2017.

[7] E. Eschner, T. Staudt, and M. Schmidt, “Sensing approach for the in-situ determination of spatter motion within PBF-LB/M,” *CIRP Annals*, vol. 71, no. 1, pp. 149–152, Jan. 2022, doi: 10.1016/J.CIRP.2022.03.005.

[8] B. C. Gross, J. L. Erkal, S. Y. Lockwood, C. Chen, and D. M. Spence, “Evaluation of 3D printing and its potential impact on biotechnology and the chemical sciences,” *Anal Chem*, vol. 86, no. 7, pp. 3240–3253, Apr. 2014, doi: 10.1021/AC403397R/ASSET/IMAGES/LARGE/AC-2013-03397R_0009.JPEG.

[9] P. A. Hooper, “Melt pool temperature and cooling rates in laser powder bed fusion,” *Addit Manuf*, vol. 22, pp. 548–559, Aug. 2018, doi: 10.1016/J.ADDMA.2018.05.032.

[10] D. Dev Singh, T. Mahender, and A. Raji Reddy, “Powder bed fusion process: A brief review,” *Mater Today Proc*, vol. 46, pp. 350–355, Jan. 2021, doi: 10.1016/J.MATPR.2020.08.415.

[11] M. Galati, “Electron beam melting process: a general overview,” *Addit Manuf*, pp. 277–301, Jan. 2021, doi: 10.1016/B978-0-12-818411-0.00014-8.

[12] D. Wang, D. Zhao, X. Liang, X. Li, and F. Lin, “Multiple stages of smoking phenomenon in electron beam powder bed fusion process,” *Addit Manuf*, vol. 66, p. 103434, Mar. 2023, doi: 10.1016/J.ADDMA.2023.103434.

[13] Z. C. Cordero, H. M. Meyer, P. Nandwana, and R. R. Dehoff, “Powder bed charging during electron-beam additive manufacturing,” *Acta Mater*, vol. 124, pp. 437–445, Feb. 2017, doi: 10.1016/J.ACTAMAT.2016.11.012.

[14] Z. Lin, S. Dabakhsh, and A. Rashid, “Developing processing windows for powder pre-heating in electron beam melting,” *J Manuf Process*, vol. 83, pp. 180–191, Nov. 2022, doi: 10.1016/J.JMAPRO.2022.08.063.

[15] S. Mirzababaei and S. Pasebani, “A Review on Binder Jet Additive Manufacturing of 316L Stainless Steel,” *Journal of Manufacturing and Materials Processing 2019, Vol. 3, Page 82*, vol. 3, no. 3, p. 82, Sep. 2019, doi: 10.3390/JMMP3030082.

[16] A. Cabo Rios, E. Hryha, E. Olevsky, and P. Harlin, “Sintering anisotropy of binder jetted 316L stainless steel: part I–sintering anisotropy,” *Powder Metallurgy*, vol. 65, no. 4, pp. 273–282, 2022, doi: 10.1080/00325899.2021.2020485.

[17] D. Apelian, “Particulate Processing (Powder Metallurgy),” *Encyclopedia of Materials: Science and Technology*, pp. 6761–6768, Jan. 2001, doi: 10.1016/B0-08-043152-6/01197-9.

[18] P. Moghimian *et al.*, “Metal powders in additive manufacturing: A review on reusability and recyclability of common titanium, nickel and aluminum alloys,” *Addit Manuf*, vol. 43, p. 102017, Jul. 2021, doi: 10.1016/J.ADDMA.2021.102017.

[19] M. A. Smirnov, M. A. Kaplan, and M. A. Sevostyanov, “Receiving finely divided metal powder by inert gas atomization,” *IOP Conf Ser Mater Sci Eng*, vol. 347, no. 1, p. 012033, Apr. 2018, doi: 10.1088/1757-899X/347/1/012033.

[20] Z. Li *et al.*, “A Review of Spatter in Laser Powder Bed Fusion Additive Manufacturing: In Situ Detection, Generation, Effects, and Countermeasures,” *Micromachines 2022, Vol. 13, Page 1366*, vol. 13, no. 8, p. 1366, Aug. 2022, doi: 10.3390/MI13081366.

[21] P. Bidare, I. Bitharas, R. M. Ward, M. M. Attallah, and A. J. Moore, “Fluid and particle dynamics in laser powder bed fusion,” *Acta Mater*, vol. 142, pp. 107–120, Jan. 2018, doi: 10.1016/j.actamat.2017.09.051.

[22] S. Ly, A. M. Rubenchik, S. A. Khairallah, G. Guss, and M. J. Matthews, “Metal vapor micro-jet controls material redistribution in laser powder bed fusion additive manufacturing OPEN”, doi: 10.1038/s41598-017-04237-z.

[23] A. Raza, C. Pauzon, S. Dubiez-Le Goff, and E. Hryha, “Effect of processing gas on spatter generation and oxidation of TiAl6V4 alloy in laser powder bed fusion process,” *Appl Surf Sci*, vol. 613, p. 156089, Mar. 2023, doi: 10.1016/J.APSUSC.2022.156089.

[24] C. Pauzon *et al.*, “Effect of helium as process gas on laser powder bed fusion of Ti-6Al-4V studied with operando diffraction and radiography,” *European Journal of Materials*, vol. 2, no. 1, pp. 422–435, Dec. 2022, doi: 10.1080/26889277.2022.2081622.

[25] A. Raza, C. Schwerz, C. Pauzon, L. Nyborg, and E. Hryha, “Effect of layer thickness on spatters oxidation of Hastelloy X alloy during powder bed fusion-laser beam processing,” *Powder Technol*, vol. 422, May 2023, doi: 10.1016/j.powtec.2023.118461.

[26] Z. Chen, A. Raza, and E. Hryha, “Influence of part geometry on spatter formation in laser powder bed fusion of Inconel 718 alloy revealed by optical tomography,” *J Manuf Process*, vol. 81, pp. 680–695, Sep. 2022, doi: 10.1016/j.jmapro.2022.07.031.

[27] T. Fiegl, M. Franke, A. Raza, E. Hryha, and C. Körner, “Effect of AlSi10Mg0.4 long-term reused powder in PBF-LB/M on the mechanical properties,” *Mater Des*, vol. 212, Dec. 2021, doi: 10.1016/j.matdes.2021.110176.

[28] A. Raza *et al.*, “Degradation of AlSi10Mg powder during laser based powder bed fusion processing,” *Mater Des*, vol. 198, Jan. 2021, doi: 10.1016/j.matdes.2020.109358.

[29] H. Gruber, M. Henriksson, E. Hryha, and L. Nyborg, “Effect of Powder Recycling in Electron Beam Melting on the Surface Chemistry of Alloy 718 Powder,” *Metall Mater Trans A Phys Metall Mater Sci*, vol. 50, no. 9, pp. 4410–4422, Sep. 2019, doi: 10.1007/s11661-019-05333-7.

[30] H. Gruber, C. Luchian, E. Hryha, and L. Nyborg, “Effect of Powder Recycling on Defect Formation in Electron Beam Melted Alloy 718,” *Metall Mater Trans A Phys Metall Mater Sci*, vol. 51, no. 5, pp. 2430–2443, May 2020, doi: 10.1007/s11661-020-05674-8.

[31] Y. Sun, M. Aindow, and R. J. Hebert, “The effect of recycling on the oxygen distribution in Ti-6Al-4V powder for additive manufacturing,” *Materials at High Temperatures*, vol. 35, no. 1–3, pp. 217–224, May 2018, doi: 10.1080/09603409.2017.1389133.

[32] J. Raplee *et al.*, “Thermographic Microstructure Monitoring in Electron Beam Additive Manufacturing OPEN,” 2017, doi: 10.1038/srep43554.

[33] A. Raza, E. Hryha, C. Koerner, and M. Markl, “Characterization of spatter and sublimation in alloy 718 during electron beam melting materials Characterization of Spatter and Sublimation in Alloy 718 during Electron Beam Melting,” 2021, doi: 10.3390/ma14205953.

[34] V. Petrovic and R. Niñerola, “Powder recyclability in electron beam melting for aeronautical use,” *Aircraft Engineering and Aerospace Technology*, vol. 87, no. 2, pp. 147–155, Mar. 2015, doi: 10.1108/AEAT-11-2013-0212.

[35] A. Mostafaei *et al.*, “Binder jet 3D printing—Process parameters, materials, properties, modeling, and challenges,” *Prog Mater Sci*, vol. 119, p. 100707, Jun. 2021, doi: 10.1016/J.PMATSCI.2020.100707.

[36] K. Janzen, K. J. Kallies, L. Waalkes, P. Imgrund, and C. Emmelmann, “Influence of Different Powder Conditioning Strategies on Metal Binder Jetting with Ti-6Al-4V,” *Materials 2024, Vol. 17, Page 750*, vol. 17, no. 3, p. 750, Feb. 2024, doi: 10.3390/MA17030750.

[37] K. Janzen, K. J. Kallies, L. Waalkes, P. Imgrund, and C. Emmelmann, “Recycling of Ti-6Al-4V Powder in Metal Binder Jetting,” *Journal of the Japan Society of Powder and Powder Metallurgy*, vol. 72, no. Supplement, pp. S353–S360, Mar. 2025, doi: 10.2497/JJSPM.15A-T7-04.

[38] K. Zissel, E. Bernardo Quejido, T. Deckers, P. Forêt, and E. Hryha, “Binder Jetting-Reusability of 17-4 PH Stainless Steel Powder,” in *Proceedings of the World PM 2022 Congress and Exhibition*, Lyon, France, 2022, pp. 9–13.

[39] S. Mirzababaei, B. K. Paul, and S. Pasebani, “Metal Powder Recyclability in Binder Jet Additive Manufacturing,” *JOM*, vol. 72, doi: 10.1007/s11837-020-04258-6.

[40] A. Barhoum and M. Luisa García-Betancourt, “Physicochemical characterization of nanomaterials: Size, morphology, optical, magnetic, and electrical properties,” in *Emerging Applications of Nanoparticles and Architectural Nanostructures: Current Prospects and Future Trends*, Elsevier Inc., 2018, pp. 279–304. doi: 10.1016/B978-0-323-51254-1.00010-5.

[41] O. Johari and S. Bhattacharyya, “The application of scanning electron microscopy for the characterization of powders,” *Powder Technol*, vol. 2, no. 6, pp. 335–348, Sep. 1969, doi: 10.1016/0032-5910(69)80026-4.

[42] F. A. Stevie and C. L. Donley, “Introduction to x-ray photoelectron spectroscopy,” *Journal of Vacuum Science & Technology A: Vacuum, Surfaces, and Films*, vol. 38, no. 6, Dec. 2020, doi: 10.1116/6.0000412.

[43] A. B. Spierings, M. Voegtlin, T. Bauer, and K. Wegener, “Powder flowability characterisation methodology for powder-bed-based metal additive manufacturing,” *Progress in Additive Manufacturing*, vol. 1, no. 1–2, pp. 9–20, Jun. 2016, doi: 10.1007/s40964-015-0001-4.

[44] L. Nyborg, A. Nylund, and I. Olefjord, “Thickness determination of oxide layers on spherically-shaped metal powders by ESCA,” *Surface and Interface Analysis*, vol. 12, no. 2, pp. 110–114, 1988, doi: 10.1002/sia.740120209.

[45] C. Oikonomou, E. Hryha, and L. Nyborg, “Development of methodology for surface analysis of soft magnetic composite powders,” in *Surface and Interface Analysis*, Aug. 2012, pp. 1166–1170. doi: 10.1002/sia.3848.